Photochemical CO_2 Capture and Release in Water Enabled By Photoacid Under Visible Light

Hyowon Seo and T. Alan Hatton

Department of Chemical Engineering, Massachusetts Institute of Technology, Cambridge, MA 02139, USA

tahatton@mit.edu

Abstract

The urgency to address climate change and its environmental consequences demands the development of effective carbon capture technologies. The relationship between rising global temperatures and increased atmospheric CO_2 levels necessitates innovative approaches for mitigating this critical issue. Here, we present a novel photochemical strategy utilizing photoacids in an aqueous bicarbonate buffer system for reversible carbon capture and release. We investigated the photochemical modulation of hydrophilic pyranine as a model photoacid, showcasing its ability to facilitate the capture and release CO_2. Control experiments provided evidence of the photoacid effect and its contribution to CO_2 release, complemented by the photothermal effect. Cyclic experiments demonstrate the efficiency and reliability of the photochemical carbon capture strategy across multiple cycles. In addition, we explored the potential use of meta-stable state photoacids for this purpose. This research introduces possibilities for the advancement of photochemical carbon capture systems, offering promising avenues for addressing the challenges associated with climate change.

The increasing climate change and associated environmental concerns mandate the need for viable solutions.[1] With the planet's temperature having surged by 1.1 °C since the commencement of the industrial

revolution, a direct correlation has been established between this temperature escalation and the surge in atmospheric CO_2 levels, currently reaching 417 parts per million[2] due to anthropogenic carbon emissions arising from the combustion of fossil fuels.[3] Consequently, it is imperative to address this issue and seek effective solutions. In order to establish effective carbon management, the development of highly efficient and economically viable carbon capture technologies assumes pivotal significance.[4]

The utilization of aqueous amine solutions through thermal-swing processes is one of the most mature technologies for carbon capture.[5] However, despite its maturity, there are some limitations associated with thermal amine capture, including high energy consumption and environmental concerns stemming from the volatility of amines.[6–10] These limitations have impeded its wider deployment in various industry sectors as well as direct air capture of CO_2. Recently, electrochemical carbon capture has emerged as a promising alternative to traditional thermal amine capture.[11–14] Unlike thermal-swing processes, electrochemical systems offer advantages such as reduced energy consumption and compatibility with renewable energy sources. By harnessing the power of electrochemistry, these systems provide a more environmentally friendly and economically feasible approach to carbon capture. Additionally, their decentralized operation and potential for localized carbon capture make them efficient and cost-effective solutions. In parallel, the exploration of photochemical carbon capture utilizing light directly opens new avenues for innovative carbon management strategies.

In this work, we have devised an efficient strategy for photochemical modulation of molecular photoswitches to facilitate carbon capture (Figure 1a). This approach draws inspiration from our lab's extensive work on electrochemical modulation of redox-active materials.[15–20] In electrochemical modulation, the redox-active material is activated through electrochemical reduction. The resulting electron-rich state of the material is sufficiently basic or nucleophilic to capture CO_2 from diluted sources. Subsequently, the CO_2-saturated solution undergoes electrochemical oxidation to regenerate the resting state of the redox-active material, releasing concentrated CO_2. This cyclic process effectively separates and concentrates CO_2 from the diluted source.

Building upon this concept, we have developed a parallel scheme for photochemical modulation of organic molecular photoswitches[21–23] (Figure 1a). In this scheme, the resting-state photoswitch, when kept in the dark along with a suitable absorbent (e.g., carbonate, amine, or alkaline solution), captures CO_2 from the diluted source. Upon irradiation, the CO_2-saturated solution releases concentrated CO_2 by lowering the local pH through the decreased pKa* of the excited states of the photoswitch. By blocking the light and returning to the dark, the excited states of the photoswitch revert to the ground state, effectively closing the cycle. In designing photo-swing carbon capture by photochemical modulation of photoswitches, we used a visible light photoacid and bicarbonate buffered system as an absorbent in this work (Figure 1b). The relationship between the bicarbonate buffer solution pH and pKa of the ground state and excited state of photoacid is important in the design of an efficient system. The pKa of the ground state is desired to be higher than the pH of the CO_2 saturated solution, and therefore, most photoacid remains protonated under dark conditions, while the pKa* of the excited state is desired to be lower than the pH of the CO_2 saturated solution so that the photoacid generates protons upon irradiation to release CO_2 out of the solution. During the CO_2 release step, the excited photoacid would be deprotonated and bicarbonate decomposed to CO_2 and water[16,19,20,24] under the decreased pH of the local condition. Following the CO_2 capture step, the photoacid returns back to its ground state and takes up a proton back under dark conditions. Following release of CO_2 during irradiation, with subsequent reversion of the buffer bicarbonate to carbonate ions under dark conditions, the sorbent is primed to again capture CO_2 from the dilute source.

The successful release of CO_2 through irradiation in photochemical modulation is influenced by various factors, including concentration of the protonated form of the photoacid, bicarbonate buffer concentration, quantum yield, and light intensities. Given that most reported visible light photoacids have pKa values within the range of 6 to 9,[23,25–27] the system consists of two buffering systems: the photoacid buffer and the bicarbonate buffer (pKa 6.4 and 10.3).

With a larger bicarbonate buffer concentration and minimal effect on pH changes in the ground state by the photoacid buffer, the concentration of the protonated form of the photoacid is determined by

the bicarbonate buffer concentration, partial pressure of CO_2, and the pKa value of the photoacid's ground state. Figure 1c illustrates the ratio of protonated photoacid ([PAH]) to the total amount of photoacid ($[PA]_{total}$), obtained under 15% CO_2 and varying bicarbonate buffer concentrations. For instance, with a pKa value of 7.7, the protonated form ([PAH]) comprises 0.6 of the total photoacid ($[PA]_{total}$) with a bicarbonate concentration of 100 mM. However, if the bicarbonate buffer concentration increases to 500 mM, the ratio of the protonated form ($[PAH]/[PA]_{total}$) in the ground state drops below 0.3. This reduced ratio implies a decrease in the effective concentration of the photoacid, thereby affecting its carbon capture and release capacity. Hence, a larger proportion of the protonated form in the ground state is desirable to maximize the carbon capture and release capacity.

To examine the influence of the ground state pKa, Figure 1c presents curves for different pKa values (8 in red, 9 in yellow, and 10 in purple). Higher pKa values were expected to result in reduced dependence of the protonated photoacid portion on bicarbonate concentration. Conversely, a lower pKa of 7 would lead to a lower effective concentration, while a pKa of 6 would result in most of the photoacid remaining in the deprotonated form regardless of the bicarbonate concentration. This deprotonation would significantly diminish CO_2 release capacity under light. Therefore, careful consideration of the ground state pKa is crucial during the initial design phase of photochemical carbon capture systems employing photoacids in bicarbonate buffer systems.

To generate a high-concentration aqueous solution of the photoacid for gas output, we employed pyranine,[26,28–30] a well-established hydrophilic photoswitch with a maximum solubility of 520 mM in water (Figure 1d). Pyranine has been extensively studied as a photoacid in various research fields, including sensors,[28,31] biology,[32] and optics[33,34]. Its ground state pKa is 7.7, while the excited state pKa* is 0.6[30], aligning well with our design and the pH of the bicarbonate buffer under 15% CO_2. As the excited state of pyranine has a relatively short half-life of 9 ns[28], no significant accumulation of excited states in the bulk solution is expected using the limited power of a commercial LED light source. However, we hypothesized that at a local time scale, localized concentrations could lead to the generation of CO_2 gas output. Once CO_2

gas escapes from the solution, the total dissolved inorganic carbon (DIC) content will gradually decrease over time.

The photochemical working scheme is depicted in Figure 1e. In the bicarbonate buffer, the ground state photoacid (pyranine, $\lambda_{abs,max}$ = 400 nm) is excited upon irradiation with blue light (427 nm). The excited state of the photoacid, with a pKa* value of 0.6, undergoes deprotonation within the pH range of 6 to 8 of the solution. Consequently, the released proton reduces the pH of the local environment, causing the bicarbonate ions to decompose into CO_2 and H_2O. Upon return to a dark environment, the photoswitch transitions back to the ground state, acquiring a proton from the bicarbonate ions and generating carbonate ions. These carbonate ions actively participate in capturing CO_2 from the dilute source. Through this light-dark cycle, CO_2 can be separated and concentrated.

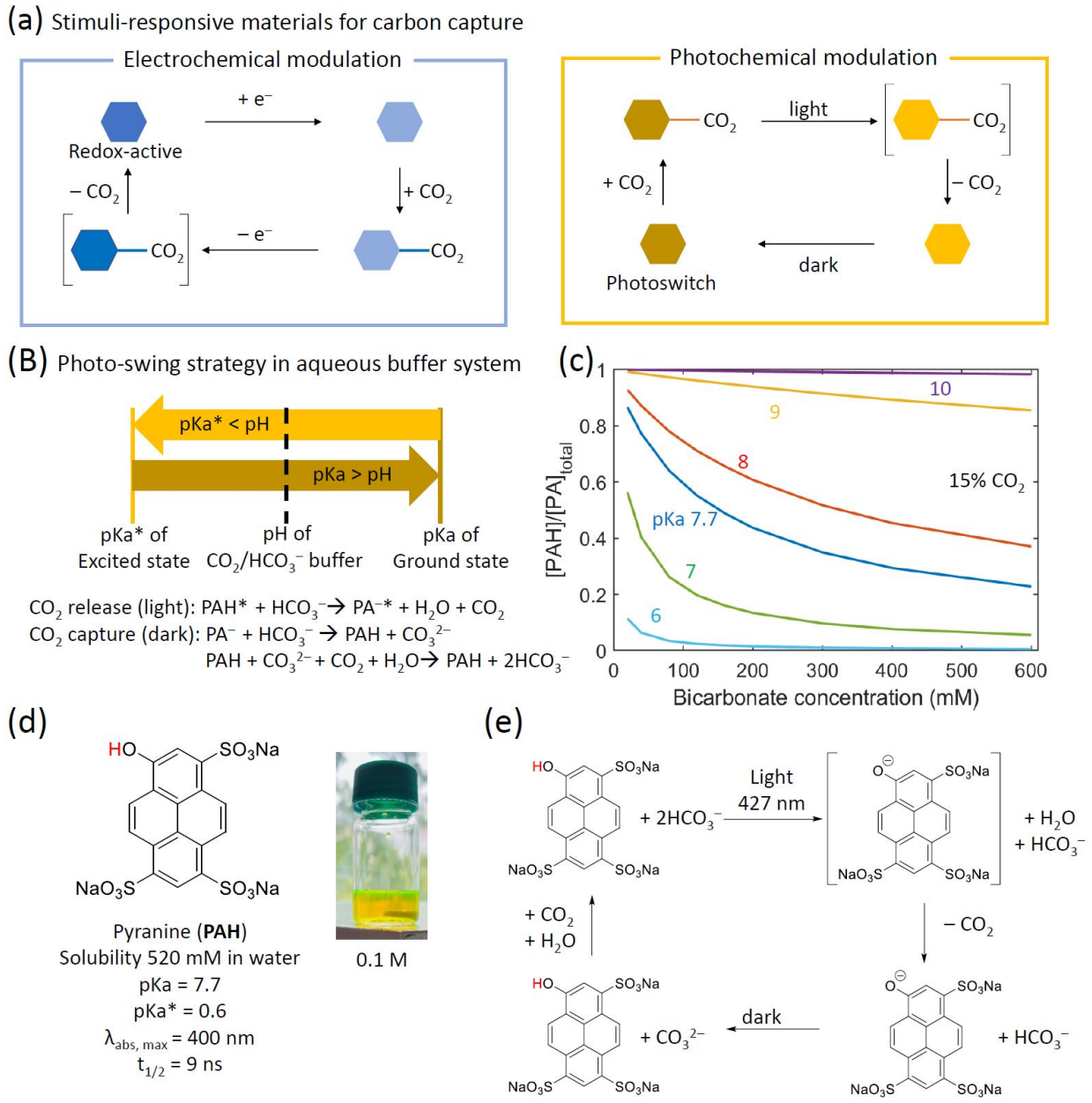

Figure 1. Photochemical CO_2 capture by a molecular photoswitch under visible light. (a) Stimuli-responsive materials for carbon capture: electrochemical modulation and photochemical modulation. (b) Photo-swing strategy of carbon capture using a molecular photoacid in an aqueous bicarbonate buffer solution. (c) Correlation between the ratio of the protonated form of the photoacid ([PAH]) and the total amount of photoacid added ($[PA]_{total}$) with varying bicarbonate concentrations in water under 15% CO_2. (d) Pyranine as a hydrophilic photoacid in water and its physicochemical properties. 0.1 M pyranine solution

is presented. (e) Working scheme illustrating the photochemical carbon capture process employing pyranine as a photoacid in bicarbonate buffer system.

A bench-scale setup was assembled to investigate CO_2 capture and release in the pyranine photoacid system under 15% CO_2 and blue LED light irradiation (Figure 2a). The setup consisted of a reaction vial containing 5 mL of the photoacid solution, with the 15% CO_2 introduced into the vial at the desired flow rate using a mass-flow controller. The solution pH was monitored by a pH probe. Gas output from the reaction vial was measured using a mass-flow meter and an IR CO_2 sensor. The reaction vial was enclosed within an aluminum photobox designed to reflect and confine the light emitted by a 45 W blue LED at 427 nm. During the reaction, the photobox was cooled using a cooling fan. The solution used in the experiments contained 100 mM of pyranine and 100 mM of potassium carbonate (K_2CO_3). Before the photoreaction, the solution was saturated with 15% CO_2. Once saturation was achieved, the reaction vial was irradiated, and the gas output was recorded. Figure 2b illustrates the observed CO_2 release under the standard conditions, where a total of 0.12 mmol of CO_2 was collected within 30 minutes (blue curve).

To confirm that the observed CO_2 release was indeed due to the photoacid effect, control experiments were conducted. In the first control experiment, the photoacid was omitted while keeping all other conditions the same. Even in the absence of the photoacid, a CO_2 release of 0.039 mmol was obtained within 30 minutes. This result was attributed to an increase in temperature caused by the irradiation, leading to reduced CO_2 solubility at higher temperatures. However, the temperature increase (35 °C) was lower than under the standard conditions due to the absence of a photoactive molecule. The temperature reached approximately 60 °C within 30 minutes under the standard conditions due to the photothermal effect of pyranine. In the second control experiment, thermal heating was applied to induce CO_2 release at 60 °C. A standard solution containing 100 mM of pyranine and 100 mM of bicarbonate, saturated with 15% CO_2,

was heated using a hot plate within an oil bath. The CO_2 output measured was 0.072 mmol within 15 minutes. These results indicated that a combination of the photoacid effect and the photothermal effect contributed to the CO_2 release. Specifically, the photoacid effect accounted for the release of 0.058 mmol of CO_2 under the standard conditions, while the remaining 0.072 mmol was attributed to the photothermal effect.

The pH variation during a series of photochemical reactions was investigated (Figure 2c). Firstly, under a nitrogen atmosphere, in the absence of CO_2 and carbonate species, the pH of the standard solution decreased from 4.1 to 3.2 within 15 minutes of blue light irradiation (Figure 2c, top). Notably, despite the ultra-short half-life (9 ns) of the excited state, a significant drop in bulk pH was observed. Although further investigations are warranted, it is hypothesized that the solvation by water molecules contributes to the pH change in this high pyranine concentration solution.[30,35–39] Secondly, a pyranine solution with an initial pH of 7 was subjected to irradiation, and the pH dynamics were monitored (Figure 2c, middle). A modest pH change from 7.1 to 7.05 was observed during the first 6 minutes of light exposure. This subtle pH variation can be attributed to the buffering effect provided by the ground state of pyranine (pKa 7.7). Thirdly, during the CO_2 release and capture step of the standard solution, the pH profile was recorded (Figure 2c, bottom). In the release step under light, a pH drop occurred within the first 10 minutes, followed by a gradual increase over the subsequent 20 minutes, consistent with the observed release of CO_2 during irradiation. Upon turning off the light, a rapid pH jump was observed, followed by a gradual pH decrease upon the introduction of 15% CO_2 at a flow rate of 50 mL/min, corresponding to the capture of CO_2 by the solution.

A control experiment involving light on and off was conducted to validate the photochemical process (Figure 2d). The standard solution, comprising 100 mM pyranine and 100 mM potassium carbonate saturated with 15% CO_2, was subjected to one minute of irradiation followed by one minute without light. Notably, a distinct pattern of gas output flow was observed during this experiment, with a sharp increase during light exposure and a corresponding decrease when the light was turned off. This outcome demonstrates the indispensable role of irradiation in CO_2 release. Moreover, the observed pattern suggests

a predominant photoacid effect rather than a photothermal effect, as photothermal effect may exhibit a gradual gas output during the light-on phase, followed by a gradual decline during the light-off phase.

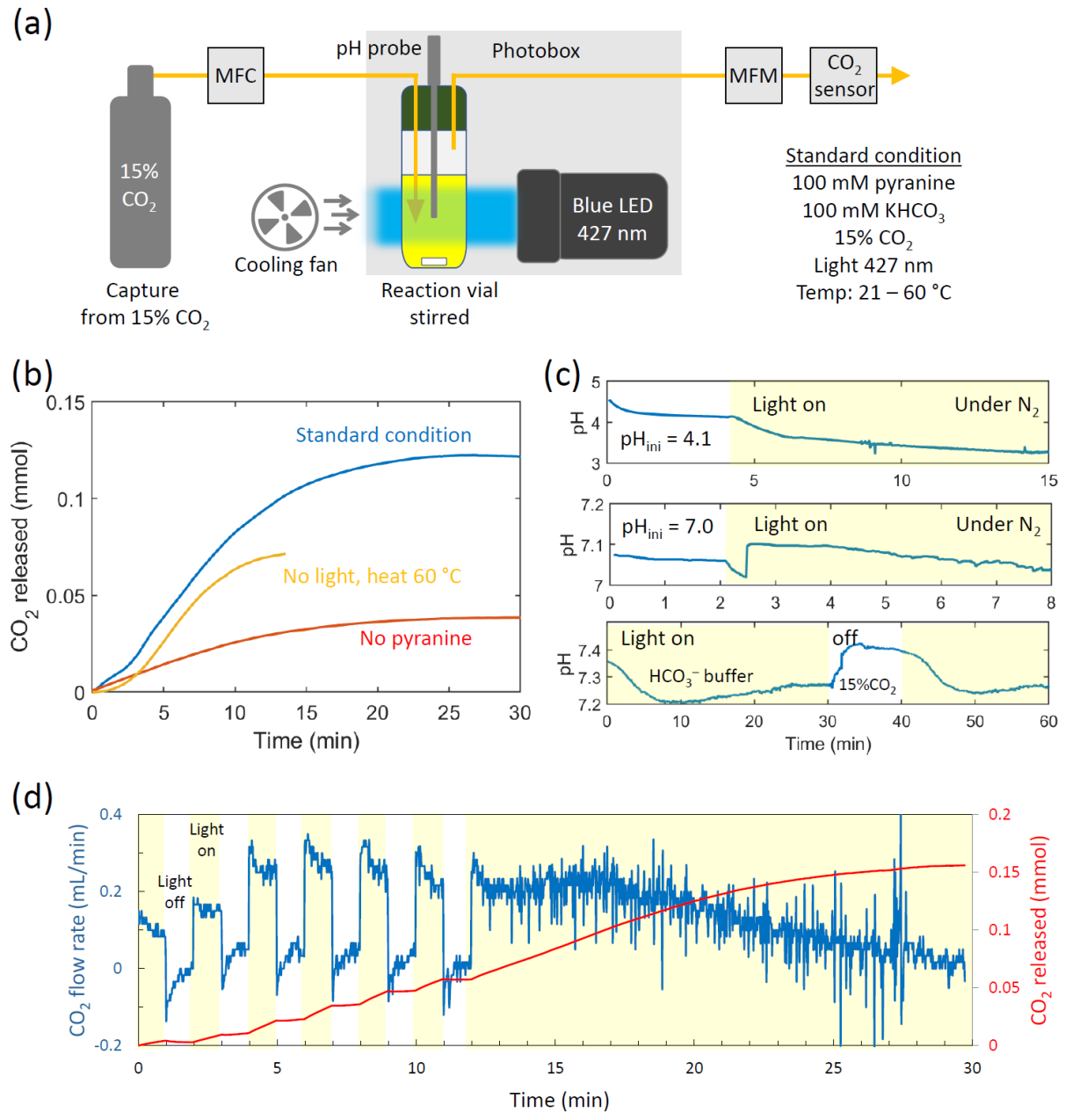

Figure 2. Photochemical release of CO_2 using pyranine photoacid system. (a) Schematic representation of the experimental setup illustrating the standard condition for photochemical CO_2 release. The reaction vial containing a pyranine solution is irradiated by a blue LED (427 nm) at room temperature. The vial is

connected to a mass-flow meter (MFM) and a CO_2 sensor. The feed gas of 15% CO_2 is supplied through a mass-flow controller (MFC). (b) CO_2 release from a 5 mL aqueous solution of 100 mM pyranine and 100 mM K_2CO_3 saturated by 15% CO_2 irradiated by a blue LED (427 nm). The plot shows the amount of released CO_2 under the standard condition (blue curve) as well as two control experiments: no pyranine present (red curve) and no light exposure, but heating to 60 °C (yellow curve). (c) (Top) pH profile of a 100 mM pyranine solution in water (initial pH 4.1) irradiated by a blue LED (427 nm) for 15 minutes. (Middle) pH profile of a 100 mM pyranine solution in water (initial pH 7.0, adjusted by KOH) irradiated by a blue LED (427 nm) for 8 minutes. (Bottom) pH profile during CO_2 release (light) step in the presence of 100 mM of K_2CO_3 saturated by 15% CO_2 followed by capture step (dark) by 15% CO_2 at a flow rate of 50 mL/min. (d) On/off studies demonstrating the effect of visible light by switching the light on and off during the photochemical process.

We performed a cyclic experiment of CO_2 capture and release utilizing the pyranine photoacid system (Figure 3a). The standard solution, consisting of 100 mM pyranine and 100 mM K_2CO_3 saturated with 15% CO_2, was prepared. The experiment involved repeated cycles of 30 minutes of irradiation for CO_2 release, followed by 10 minutes of contact with 15% CO_2 at a flow rate of 50 mL/min for CO_2 capture. The results of multiple cyclic CO_2 release are presented in Figure 3a. Over the course of 5 cycles, the amount of CO_2 released through irradiation was approximately 0.1 mmol for each cycle. To ensure the photostability of pyranine during the experiment, we performed NMR spectroscopy under the operational conditions for 5 cycles, as shown in Figure 3b.

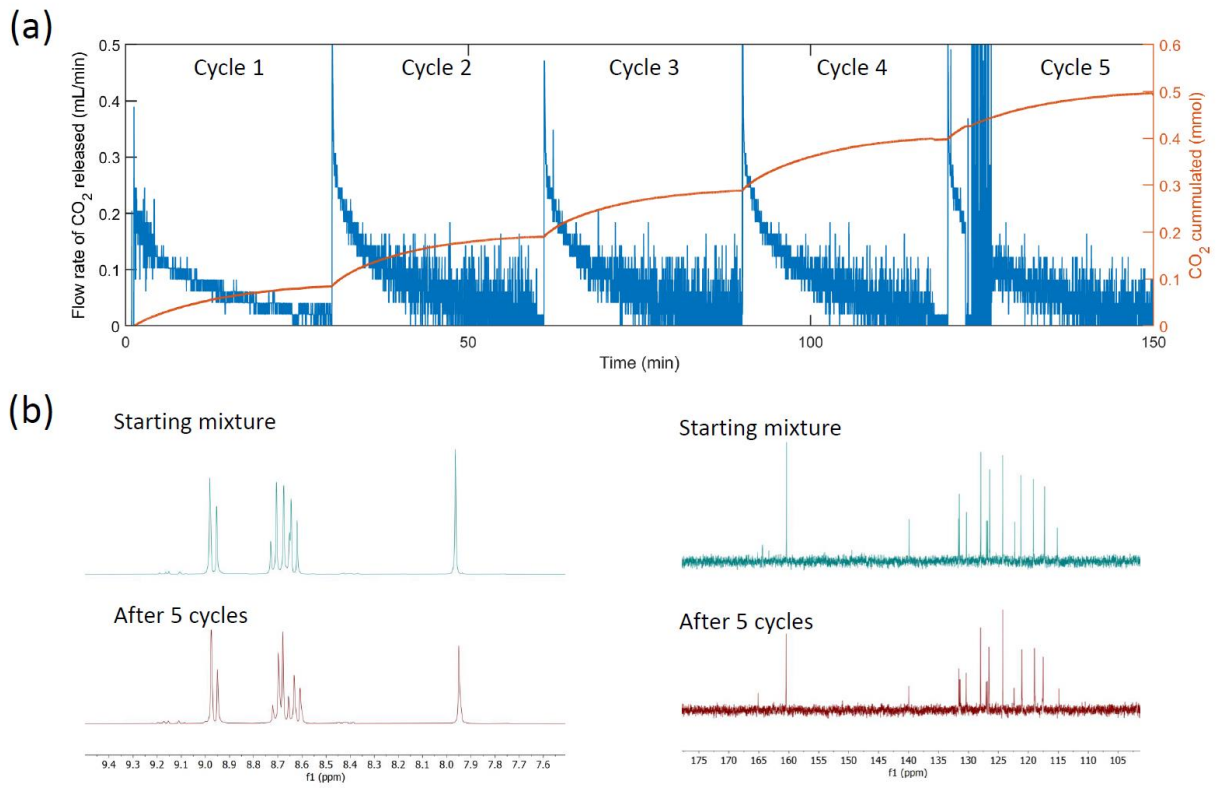

191

192 **Figure 3**. Cyclic experiments of the photochemical capture and release of CO_2 using 100 mM of pyranine
193 in water (5 mL). (a) CO_2 release profile from a 5 mL aqueous solution containing 100 mM pyranine and
194 100 mM K_2CO_3 saturated with 15% CO_2. The solution was irradiated by a blue LED (427 nm) (red curve);
195 the flow rate of CO_2 is shown in the blue curve. (b) ^{1}H-NMR and ^{13}C-NMR spectra of the starting mixture
196 and the solution after 5 cycles of the photochemical capture and release process.

197

198

199 Although CO_2 release was observed through irradiation using the pyranine photoacid system, the
200 current capacity of CO_2 released (0.13 mmol of CO_2 released per cycle using 500 mmol of pyranine) is
201 limited. We attribute this low capacity to the short half-life of the excited species in the pyranine photoacid
202 system. To address this limitation, we hypothesized that a photoacid with a longer half-life, capable of
203 accumulating excited states over time, could provide a larger capacity for CO_2 capture and release upon

irradiation. Among the reported meta-stable state photoacids (mPAH), we selected Liao's photoacid[23] as a model compound (Figure 4a). Liao's photoacid exhibits desirable values of pKa (7.8) and pKa* (1.7 - 3.2) and possesses a long half-life of 70 s.[40] Despite its extremely low solubility in water (0.19 mM),[27] we successfully obtained a 71 mM solution by incorporating 3.5 M of nicotinamide as a hydrotropic agent in water.[16,41] The photochemical working scheme of Liao's photoacid is depicted in Figure 4b. The mPAH solution, saturated with 15% CO_2, undergoes photochemical isomerization from *E* to *Z* upon irradiation. The proximity of the phenol group and C2 of the indole moiety in the *Z* conformation leads to cyclization and subsequent proton transfer. Upon returning to the dark environment, the mPAH reverts back to the *E* configuration, completing the cycle.

The measurement of pH provides evidence supporting the accumulation of excited states over time through irradiation (Figure 4c). The pH of the 71 mM mPAH in aqueous solution decreased from 5.3 to 5.0 within 3 minutes under light exposure (Figure 4c, top). Upon turning off the light, the pH gradually returned to 6.2 within 30 minutes. Subsequently, mPAH buffer system at pH 7 was irradiated and the recorded pH shows gradual decrease of pH from 7.0 to 6.85 over 15 min. pH reverted back to its starting value when the light was turned off (Figure 4c, middle). This small pH change can be attributed to the buffering effect provided by the ground state of mPAH (pKa 7.8). Measurement of pH in the presence of 100 mM of K_2CO_3 saturated under 15% CO_2 presented a gradual increase in pH while irradiated and decrease in pH under dark, which is consistent with the proposed photochemical working scheme (Figure 4c, bottom). A light on and off experiment further confirms the essential role of light in CO_2 release (Figure 4d). Although preliminary, the results indicate that the extended half-life of the excited state of Liao's photoacid provided stable CO_2 release during irradiation. In a cyclic experiment comprising 3 cycles, each cycle resulted in a CO_2 output of 0.07 mmol. Further investigations are necessary to explore potential enhancements in CO_2 release capacity using alternative strategies.

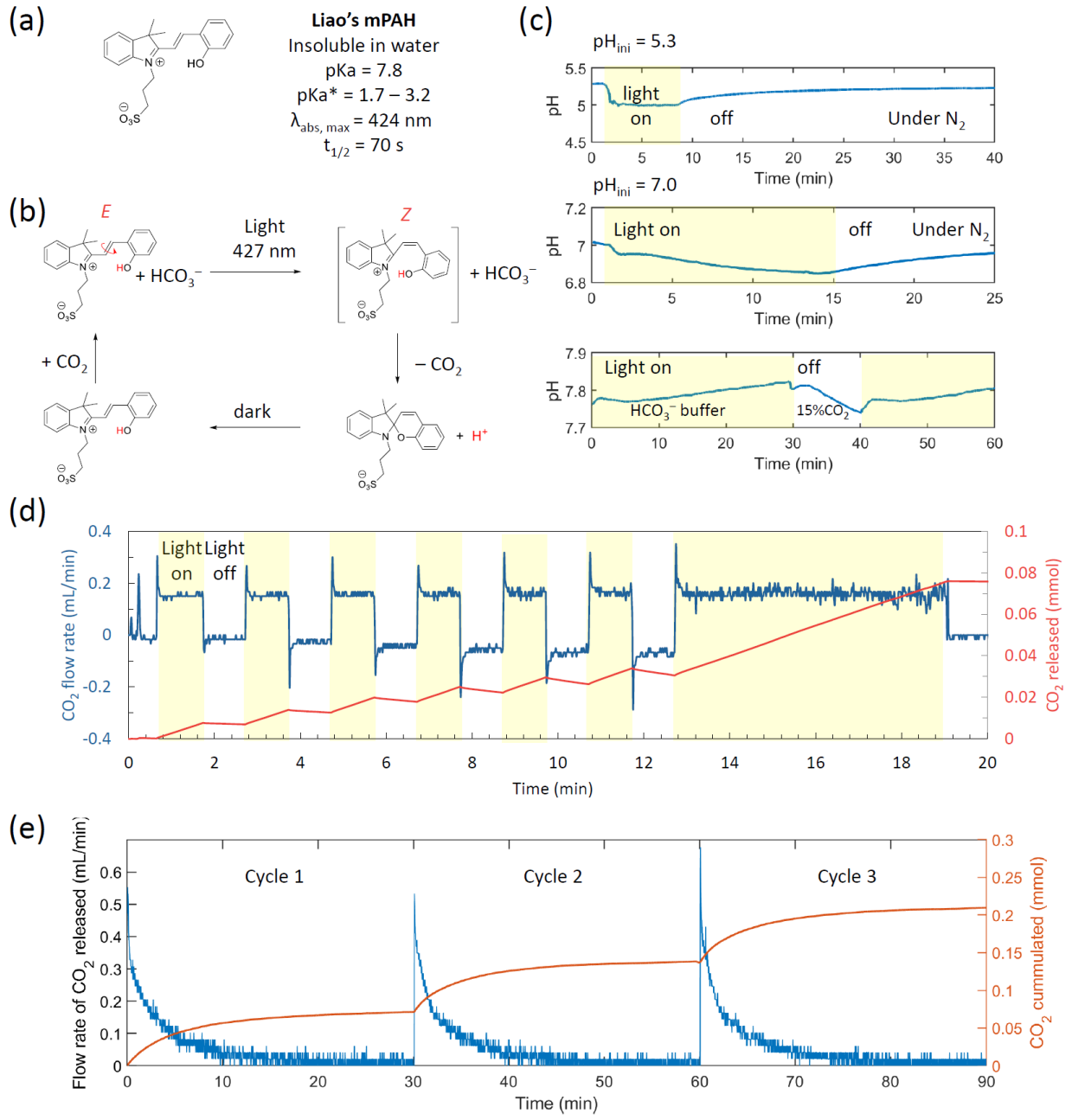

227

228 **Figure 4**. Photochemical CO_2 capture using meta-stable state photoacid (mPAH). (a) Liao's photoacid and
229 its physicochemical properties. (b) Schematic representation of the photochemical working scheme for the
230 carbon capture cycle using mPAH in water. (c) (Top) pH profile of a 71 mM mPAH solution in water
231 (initial pH 5.3) irradiated by a blue LED (427 nm) for 8 minutes. (Middle) pH profile of a 71 mM mPAH
232 solution in water (initial pH 7.0, adjusted by KOH) irradiated by a blue LED (427 nm) for 14 minutes.

(Bottom) pH profile during CO_2 release (light) step in the presence of 100 mM of K_2CO_3 saturated by 15% CO_2 followed by capture step (dark) by 15% CO_2 at a flow rate of 50 mL/min. (d) Control experiment demonstrating the effect of light by switching the light on and off. (e) Cyclic experiment of photochemical carbon capture using a 71 mM mPAH solution in a 3.5 M nicotinamide aqueous solution (5 mL).

In summary, we have developed a photochemical carbon capture strategy in an aqueous bicarbonate buffer system, utilizing the unique properties of photoacids and their response to light. Our study focused on the photochemical modulation of the hydrophilic pyranine molecule as a model system for carbon capture. Control experiments verified the contribution of the photoacid effect, along with a photothermal effect, to CO_2 release. Cyclic experiments demonstrated the feasibility of the system over 5 cycles. Additionally, we explored a meta-stable state photoacid with a longer excited state half-life, with observed stable CO_2 release upon irradiation, while the CO_2 release capacity is still limited. Future studies should consider the quantum yield of the photoacid and aim to design photoacid systems with high pKa values in the ground state. This approach will not only enhance the effective capacity of the photoacid system for carbon capture but also simplify the system by relying solely on the bicarbonate buffer, enabling better system control. Our research opens up new avenues for the development of novel photochemical carbon capture strategies. Looking ahead, future developments will aim to create photochemical systems that harness sunlight, thereby enabling energy-efficient carbon capture without the need for external energy inputs. This advancement has the potential to revolutionize the field of photo-swing carbon capture, allowing for efficient and controlled capture and release of CO_2, facilitating its further utilization or storage.

Acknowledgement

This work was partially supported jointly by the U.S. Department of Energy, Office of Science, Office of Basic Energy Sciences, Divisions of Chemical Sciences, Geosciences, and Biosciences (CSGB) and Materials Sciences and Engineering (MSE) under FWP 76830

Reference

(1) IPCC, 2021: Climate Change 2021: The Physical Science Basis. Contribution of Working Group I to the Sixth Assessment Report of the Intergovernmental Panel on Climate Change.

(2) *Greenhouse gases continued to increase rapidly in 2022*. https://www.noaa.gov/news-release/greenhouse-gases-continued-to-increase-rapidly-in-2022 (accessed 2023-06-20).

(3) Hashimoto, K. Global Temperature and Atmospheric Carbon Dioxide Concentration. In *Global Carbon Dioxide Recycling*; SpringerBriefs in Energy; Springer Singapore: Singapore, 2019; pp 5–17. https://doi.org/10.1007/978-981-13-8584-1_3.

(4) Bui, M.; Adjiman, C. S.; Bardow, A.; Anthony, E. J.; Boston, A.; Brown, S.; Fennell, P. S.; Fuss, S.; Galindo, A.; Hackett, L. A.; Hallett, J. P.; Herzog, H. J.; Jackson, G.; Kemper, J.; Krevor, S.; Maitland, G. C.; Matuszewski, M.; Metcalfe, I. S.; Petit, C.; Puxty, G.; Reimer, J.; Reiner, D. M.; Rubin, E. S.; Scott, S. A.; Shah, N.; Smit, B.; Trusler, J. P. M.; Webley, P.; Wilcox, J.; Mac Dowell, N. Carbon Capture and Storage (CCS): The Way Forward. *Energy Environ. Sci.* **2018**, *11* (5), 1062–1176. https://doi.org/10.1039/C7EE02342A.

(5) Fasihi, M.; Efimova, O.; Breyer, C. Techno-Economic Assessment of CO2 Direct Air Capture Plants. *Journal of Cleaner Production* **2019**, *224*, 957–980. https://doi.org/10.1016/j.jclepro.2019.03.086.

(6) Rheinhardt, J. H.; Singh, P.; Tarakeshwar, P.; Buttry, D. A. Electrochemical Capture and Release of Carbon Dioxide. *ACS Energy Lett.* **2017**, *2* (2), 454–461. https://doi.org/10.1021/acsenergylett.6b00608.

(7) Borhani, T. N. G.; Azarpour, A.; Akbari, V.; Wan Alwi, S. R.; Manan, Z. A. CO2 Capture with Potassium Carbonate Solutions: A State-of-the-Art Review. *International Journal of Greenhouse Gas Control* **2015**, *41*, 142–162. https://doi.org/10.1016/j.ijggc.2015.06.026.

(8) Rochelle, G. T. Amine Scrubbing for CO2 Capture. *Science* **2009**, *325* (5948), 1652–1654. https://doi.org/10.1126/science.1176731.

(9) Krzemień, A.; Więckol-Ryk, A.; Smoliński, A.; Koteras, A.; Więcław-Solny, L. Assessing the Risk of Corrosion in Amine-Based CO2 Capture Process. *Journal of Loss Prevention in the Process Industries* **2016**, *43*, 189–197. https://doi.org/10.1016/j.jlp.2016.05.020.

(10) Nguyen, T.; Hilliard, M.; Rochelle, G. T. Amine Volatility in CO2 Capture. *International Journal of Greenhouse Gas Control* **2010**, *4* (5), 707–715. https://doi.org/10.1016/j.ijggc.2010.06.003.

(11) Renfrew, S. E.; Starr, D. E.; Strasser, P. Electrochemical Approaches toward CO_2 Capture and Concentration. *ACS Catal.* **2020**, *10* (21), 13058–13074. https://doi.org/10.1021/acscatal.0c03639.

(12) Sharifian, R.; Wagterveld, R. M.; Digdaya, I. A.; Xiang, C.; Vermaas, D. A. Electrochemical Carbon Dioxide Capture to Close the Carbon Cycle. *Energy Environ. Sci.* **2021**, *14* (2), 781–814. https://doi.org/10.1039/D0EE03382K.

(13) Rahimi, M.; Khurram, A.; Hatton, T. A.; Gallant, B. Electrochemical Carbon Capture Processes for Mitigation of CO_2 Emissions. *Chem. Soc. Rev.* **2022**, *51* (20), 8676–8695. https://doi.org/10.1039/D2CS00443G.
(14) Liu, Y.; Lucas, É.; Sullivan, I.; Li, X.; Xiang, C. Challenges and Opportunities in Continuous Flow Processes for Electrochemically Mediated Carbon Capture. *iScience* **2022**, *25* (10), 105153. https://doi.org/10.1016/j.isci.2022.105153.
(15) Voskian, S.; Hatton, T. A. Faradaic Electro-Swing Reactive Adsorption for CO_2 Capture. *Energy Environ. Sci.* **2019**, *12* (12), 3530–3547. https://doi.org/10.1039/C9EE02412C.
(16) Seo, H.; Hatton, T. A. Electrochemical Direct Air Capture of CO2 Using Neutral Red as Reversible Redox-Active Material. *Nat Commun* **2023**, *14* (1), 313. https://doi.org/10.1038/s41467-023-35866-w.
(17) Seo, H.; Rahimi, M.; Hatton, T. A. Electrochemical Carbon Dioxide Capture and Release with a Redox-Active Amine. *J. Am. Chem. Soc.* **2022**, *144* (5), 2164–2170. https://doi.org/10.1021/jacs.1c10656.
(18) Diederichsen, K. M.; Liu, Y.; Ozbek, N.; Seo, H.; Hatton, T. A. Toward Solvent-Free Continuous-Flow Electrochemically Mediated Carbon Capture with High-Concentration Liquid Quinone Chemistry. *Joule* **2022**, *6* (1), 221–239. https://doi.org/10.1016/j.joule.2021.12.001.
(19) Kim, S.; Nitzsche, M. P.; Rufer, S. B.; Lake, J. R.; Varanasi, K. K.; Hatton, T. A. Asymmetric Chloride-Mediated Electrochemical Process for CO_2 Removal from Oceanwater. *Energy Environ. Sci.* **2023**, 10.1039.D2EE03804H. https://doi.org/10.1039/D2EE03804H.
(20) Rahimi, M.; Catalini, G.; Puccini, M.; Hatton, T. A. Bench-Scale Demonstration of CO_2 Capture with an Electrochemically Driven Proton Concentration Process. *RSC Adv.* **2020**, *10* (29), 16832–16843. https://doi.org/10.1039/D0RA02450C.
(21) Zivic, N.; Kuroishi, P. K.; Dumur, F.; Gigmes, D.; Dove, A. P.; Sardon, H. Recent Advances and Challenges in the Design of Organic Photoacid and Photobase Generators for Polymerizations. *Angewandte Chemie International Edition* **2019**, *58* (31), 10410–10422. https://doi.org/10.1002/anie.201810118.
(22) Kagel, H.; Frohme, M.; Glökler, J. Photoacids in Biochemical Applications. *Journal of Cellular Biotechnology* **2018**, *4* (1–2), 23–30. https://doi.org/10.3233/JCB-189004.
(23) Liao, Y. Design and Applications of Metastable-State Photoacids. *Acc. Chem. Res.* **2017**, *50* (8), 1956–1964. https://doi.org/10.1021/acs.accounts.7b00190.
(24) Rahimi, M.; Catalini, G.; Hariharan, S.; Wang, M.; Puccini, M.; Hatton, T. A. Carbon Dioxide Capture Using an Electrochemically Driven Proton Concentration Process. *Cell Reports Physical Science* **2020**, *1* (4), 100033. https://doi.org/10.1016/j.xcrp.2020.100033.
(25) Emond, M.; Le Saux, T.; Maurin, S.; Baudin, J.-B.; Plasson, R.; Jullien, L. 2-Hydroxyazobenzenes to Tailor PH Pulses and Oscillations with Light. *Chem. Eur. J.* **2010**, *16* (29), 8822–8831. https://doi.org/10.1002/chem.201000541.
(26) Lennox, J. C.; Danilov, E. O.; Dempsey, J. L. Delayed Photoacidity Produced through the Triplet–Triplet Annihilation of a Neutral Pyranine Derivative. *Phys. Chem. Chem. Phys.* **2019**, *21* (29), 16353–16358. https://doi.org/10.1039/C9CP02929J.
(27) Berton, C.; Busiello, D. M.; Zamuner, S.; Scopelliti, R.; Fadaei-Tirani, F.; Severin, K.; Pezzato, C. Light-Switchable Buffers. *Angew Chem Int Ed* **2021**, *60* (40), 21737–21740. https://doi.org/10.1002/anie.202109250.
(28) Nandi, R.; Amdursky, N. The Dual Use of the Pyranine (HPTS) Fluorescent Probe: A Ground-State PH Indicator and an Excited-State Proton Transfer Probe. *Acc Chem Res* **2022**, *55* (18), 2728–2739. https://doi.org/10.1021/acs.accounts.2c00458.
(29) Spry, D. B.; Goun, A.; Bell, C. B.; Fayer, M. D. Identification and Properties of the La1 and Lb1 States of Pyranine. *The Journal of Chemical Physics* **2006**, *125* (14), 144514. https://doi.org/10.1063/1.2358685.
(30) Awasthi, A. A.; Singh, P. K. Proton Transfer Reaction Dynamics of Pyranine in DMSO/Water Mixtures. *ChemPhysChem* **2018**, *19* (2), 198–207. https://doi.org/10.1002/cphc.201701133.

(31) Chandra, A.; Prasad, S.; Iuele, H.; Colella, F.; Rizzo, R.; D'Amone, E.; Gigli, G.; del Mercato, L. L. Highly Sensitive Fluorescent PH Microsensors Based on the Ratiometric Dye Pyranine Immobilized on Silica Microparticles. *Chemistry – A European Journal* **2021**, *27* (53), 13318–13324. https://doi.org/10.1002/chem.202101568.
(32) Clement, N. R.; Gould, J. M. Pyranine (8-Hydroxy-1,3,6-Pyrenetrisulfonate) as a Probe of Internal Aqueous Hydrogen Ion Concentration in Phospholipid Vesicles. *Biochemistry* **1981**, *20* (6), 1534–1538. https://doi.org/10.1021/bi00509a019.
(33) Development of an Optical Fiber Fluorescence Setup for In-Situ PAHs Detection in Porous Media. Application to Pyranine Transport in Sand Columns. *International Journal of Environmental Analytical Chemistry* **1997**. https://doi.org/10.1080/03067319708030493.
(34) Gan, B. S.; Krump, E.; Shrode, L. D.; Grinstein, S. Loading Pyranine via Purinergic Receptors or Hypotonic Stress for Measurement of Cytosolic PH by Imaging. *American Journal of Physiology-Cell Physiology* **1998**, *275* (4), C1158–C1166. https://doi.org/10.1152/ajpcell.1998.275.4.C1158.
(35) Spies, C.; Finkler, B.; Acar, N.; Jung, G. Solvatochromism of Pyranine-Derived Photoacids. *Phys. Chem. Chem. Phys.* **2013**, *15* (45), 19893–19905. https://doi.org/10.1039/C3CP53082E.
(36) Mohammed, O. F.; Dreyer, J.; Magnes, B.-Z.; Pines, E.; Nibbering, E. T. J. Solvent-Dependent Photoacidity State of Pyranine Monitored by Transient Mid-Infrared Spectroscopy. *ChemPhysChem* **2005**, *6* (4), 625–636. https://doi.org/10.1002/cphc.200400510.
(37) Hoberg, C.; Talbot, J. J.; Shee, J.; Ockelmann, T.; Mahanta, D. D.; Novelli, F.; Head-Gordon, M.; Havenith, M. Caught in the Act: Real-Time Observation of the Solvent Response That Promotes Excited-State Proton Transfer in Pyranine. *Chem. Sci.* **2023**, *14* (15), 4048–4058. https://doi.org/10.1039/D2SC07126F.
(38) Chiariello, M. G.; Raucci, U.; Donati, G.; Rega, N. Water-Mediated Excited State Proton Transfer of Pyranine–Acetate in Aqueous Solution: Vibrational Fingerprints from Ab Initio Molecular Dynamics. *J Phys Chem A* **2021**, *125* (17), 3569–3578. https://doi.org/10.1021/acs.jpca.1c00692.
(39) Mondal, S. K.; Sahu, K.; Ghosh, S.; Sen, P.; Bhattacharyya, K. Excited-State Proton Transfer from Pyranine to Acetate in γ-Cyclodextrin and Hydroxypropyl γ-Cyclodextrin. *J. Phys. Chem. A* **2006**, *110* (51), 13646–13652. https://doi.org/10.1021/jp063436v.
(40) Shi, Z.; Peng, P.; Strohecker, D.; Liao, Y. Long-Lived Photoacid Based upon a Photochromic Reaction. *J. Am. Chem. Soc.* **2011**, *133* (37), 14699–14703. https://doi.org/10.1021/ja203851c.
(41) Coffman, R. E.; Kildsig, D. O. Effect of Nicotinamide and Urea on the Solubility of Riboflavin in Various Solvents. *Journal of Pharmaceutical Sciences* **1996**, *85* (9), 951–954. https://doi.org/10.1021/js960012b.